Rectangular Arrangement of Se-Ring Clusters on Graphite Surface and Their Structural Transformation

Sci. Rep. RITU A39 (1993) pp. 57-62
No. 1, December 1993

Rectangular Arrangement of Se-Ring Clusters on Graphite Surface and Their Structural Transformation *

Ryszard Czajka[a] , Bing-Lin Gu [a, b] , Jing-Zhi Yu [a], Kaoru Ohno [a], Yoshiyuki Kawazoe [a], Atsuo Kasuya [a] and Yuichiro Nishina [a]

[a] *Institute for Materials Research, Tohoku University, Sendai 980, Japan*
[b] *Department of Physics, Tsinghua University, Beijing, 100084, China*

(Received November 30, 1993)

Ring-type Se clusters have been deposited on the C-plane of a graphite crystal and examined by STM images which were found to consist of 0.72nm×0.85nm rectangular lattices with individual molecules of 0.53nm in diameter. Se ring-type clusters sitting on each lattice point are most probably 6-membered. The STM images were taken with the bias voltage V_T between probe vs. sample as a parameter. For -0.7V < V_T <+0.7V the patterns of the rectangular lattice remains similar, but an order-disorder transition takes place at -0.065V; whereas V_T at -0.7V, the regular arrangement suddenly collapses to a random distribution of larger clusters consisting of their diameter in a range up to 5nm. The process of the structural change in the lattice system is not reversible with respect to the bias voltage. These experimental results are well explained by first-principles theoretical calculation on the structure and electronic properties of Se cluster using the DV-SCM method.

KEYWORDS: Se cluster, STM study, ring molecule, DV-SCM method, electronic properties

1. Introduction

Nano-structured systems composed of metallic or non-metallic clusters as well as artificially created low-dimensional materials have been intensively studied[1] because of their new and interesting properties and subsequent application perspectives. Group VI elements, e.g. selenium and sulfur, are known to form ring-type clusters[2),3)], and it is expected that they may create two-dimensionally ordered arrays at the early stage of deposition onto substrates[4)], though a lattice matching condition (usually encountered in the heteroepitaxial growth) has been a strong limitation in creating the artificially stacked layered structures. This difficulty, however, can be overcome if the interface bonding between clusters and the substrate has a van der Waals character. The layered materials highly oriented pyrolytic graphite (HOPG) or the transition metal dichalcogenides seem to be more suitable for these purposes. Using a Scanning Tunneling Microscope (STM)[5)], we may not only observe these artificially created nanometer scale structures but also perform some modifications and manipulations on individual molecules/clusters.[6)-8)] It is possible to apply first-principles calculation to analyze the presently observed phenomena, since they are actually atomic procedures measured directly by STM. The fundamental ideas of the structure of Se clusters and transformation processes of them are given based on the present calculation using DV-SCM method. The optimized structure by the DV-SCM method agrees well with the experimental result, and the observed order-disorder transition is explained quantitatively.

2. Experimental

Pure selenium material (99.999% purity) was dissolved in CS_2 and subsequently left for very slow evaporation of solvent[9)]. The remaining powder deep orange or red in color was taken off from the walls of a solution container and used for thermal evaporation. This selenium material was evaporated in the vacuum of 5×10^{-4}Pa from a tungsten boat very slowly at about 450K onto the HOPG substrates from 1 up to 30 minutes. Our best samples with regular arrays of clusters were obtained for deposition times in the range 10 to 15 minutes. The evaporation dose and rate may be critical to form two dimensional arrays of ring clusters because the interaction between rings easily convert them into chains which are more stable form of Se. The samples immediately after the deposition were transferred to the STM stage of Nanoscope II and measured in air. The instrument was calibrated using HOPG as a reference. Raman spectra of much thicker films grown from the same Se sample showed a broad peak at 250cm^{-1} indicating that the sample consists of ring molecules rather than the chains[10)]. According to mass spectral analysis major constituents of Se vapor are Se_5, Se_6, Se_7 and Se_8 clusters. In particular work by Mhlbach et al.[11)] showed that Se_6 was the dominant component in the temperature range of evaporation between 430K and 460K.

3. Results and discussion

Typical STM images of selenium molecules deposited on HOPG are shown in Figs. 1a-1f.

Figure 1a shows 30×30nm^2 STM image measured with a positive bias (+0.706V at the sample relative to the probe). It shows a regular arrangements of evaporated clusters with eight domains of different lattice orientations with respect to the crystallographic axes of HOPG substrate. The grain boundaries are developed. Figures 1b and 1c represent 7×7nm^2 STM images of single domain and its autocorrelation pattern, respectively. The pattern indicates regular rectangular structure with the lattice constants 0.72nm and 0.85nm. The molecules packed in the vicinity of grain boundaries are shown in Fig.1d. These features are reproducible for the different

*IMR, Report No. 1951

samples e.g. in Fig.1e where the monomolecular defects are seen additionally. The changes in the intermolecular distances near the grain boundaries in the absence of other molecules are observed in Fig.1f.

we have observed one monolayer of selenium ring-type molecules with the ring planes parallel to the HOPG substrate surface. They are bound by weak van der Waals forces. However it is difficult to state how many atoms

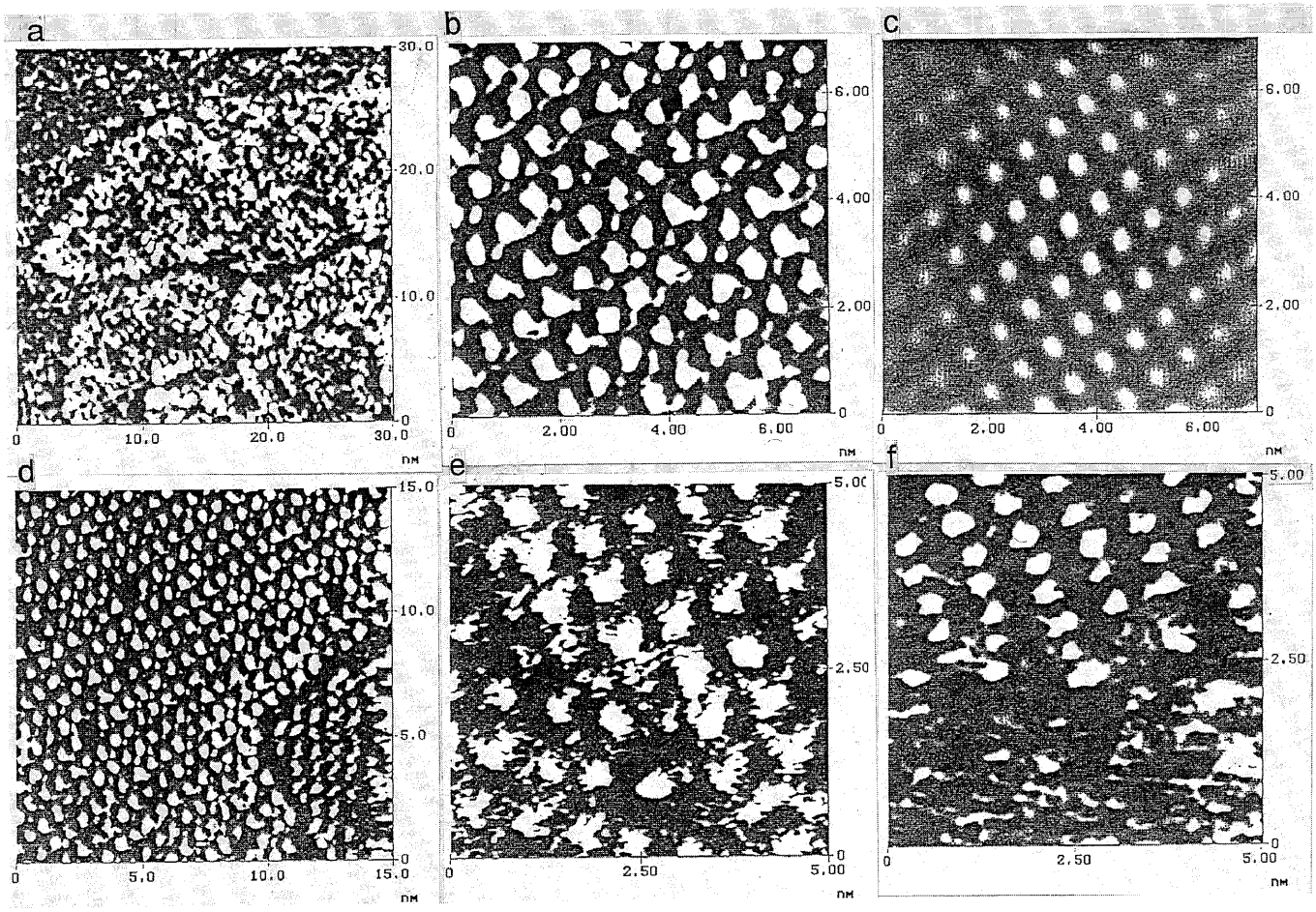

Figure 1. STM images of selenium molecules arrays on HOPG substrate: (a) $30\times30nm^2$ with domain type structures; +0.706V, 0.34nm, (b) $10\times10nm^2$ array of Se-molecules, (c) autocorrelation pattern of (b), (d) 15×15 nm^2 with monomolecular defects, (e) $5\times5nm^2$ molecules at the domain boundary and (f) $5\times5nm^2$ Se-molecules arrangement at artificially induced domain boundary.

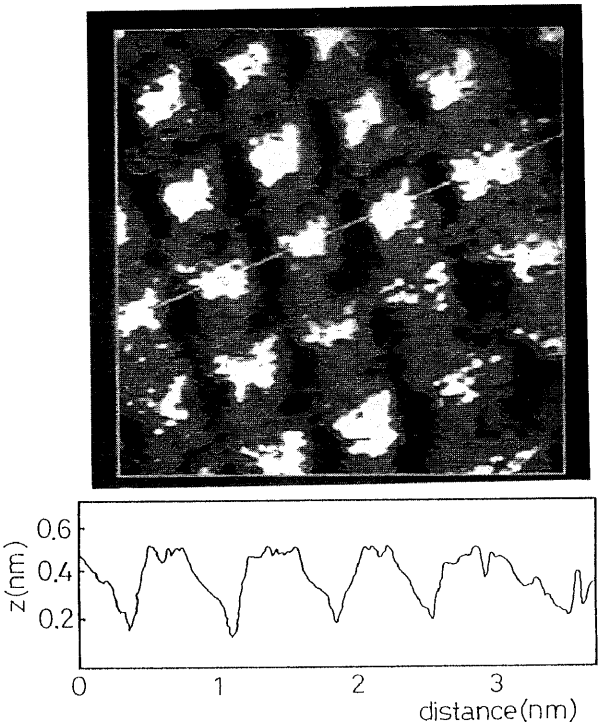

Figure 2. STM image of $4\times4nm^2$ Se-molecules array with the cross-section along the line marked on STM image(see right).

The higher magnification of these molecular crystal structure is shown in Fig.2 together with the cross-section taken along the line marked in STM image. The average diameter of the molecules is 0.53nm and the height is about 0.28nm. The diameter of individual objects (0.53nm) is comparable to 0.526nm found for Se_8 rings in a monoclinic crystal. The lattice constants (0.72nm×0.85nm) coincide with three times of binary and bisectric distances of the hexagon in graphite.

Figures 3a and 3b show the geometrical model of selenium 6- and 8-membered molecule arrays on HOPG as deduced from the present STM data. No steps were observed at the grain boundaries nor inside the grains. We, therefore, identified that these structures were due to two-dimensional arrays of nanoclusters. In short,

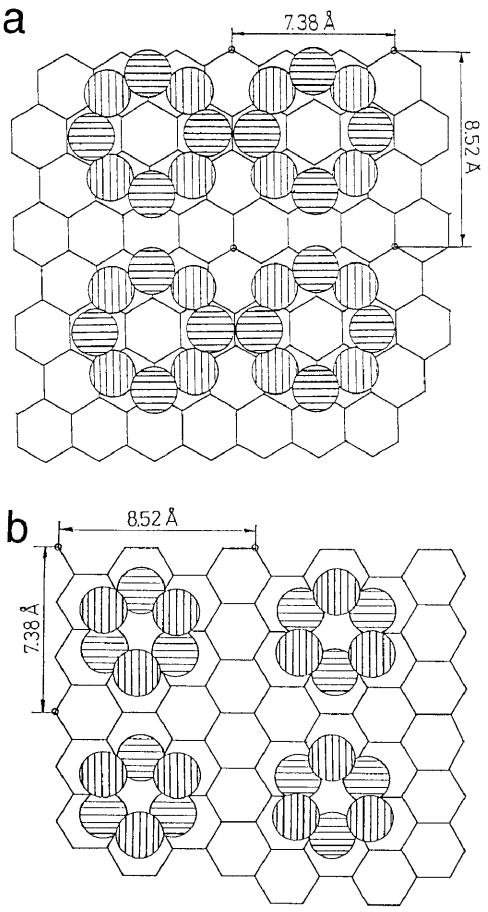

Figure 3. Geometric model of the configurations for (a) the 6-membered and (b) the 8-membered of Se rings on HOPG surface. (Se molecules are crown type.)

constitute each ring — 5, 6, 7 or 8 atoms — because we could not obtain a better resolution on the STM image of individual molecules.

On the other hand, within the STM data error of 0.05nm, it is impossible to decide which type of ring we observe on the base of the geometrical parameter data[4]. Further investigations are necessary to solve this problem. Later, our theoretical calculation suggests that the 6-membered ring type molecule might be dominant and the mixture of 5- up to 8-membered ring type molecules can be considered because of the different shape of observed species.

The modification of these structures was performed by increasing tunnel current and changing the bias voltage. By increasing tunnel current (pushing the tip towards the surface), it was possible to remove some molecules from their ordered arrays. We could not observe clear atomic resolution of the substrate but only one monomolecular step 0.28nm in height. The intermolecular distances close to the new array boundary were increased as shown in Fig.lf, indicating the existence of intermolecular interactions stronger than the interaction by the van der Waals force with the HOPG surface. This results show that both cluster-cluster and cluster-substrate interactions are important for forming nanocluster lattice system. Similar non-hexagonal superlattices were observed by Ansellmetti et al.[12] on the surfacess of stage-1 Rb and Cs grahpite interaction com-

Figure 4. STM image of $10\times10nm^2$ area taken for different tunnel voltage biases: (a) +0.7V, (b) +0.15V, (c) +0.065V, (d) -0.065V, (e) -0.30V and (f) -0.7V(see below).

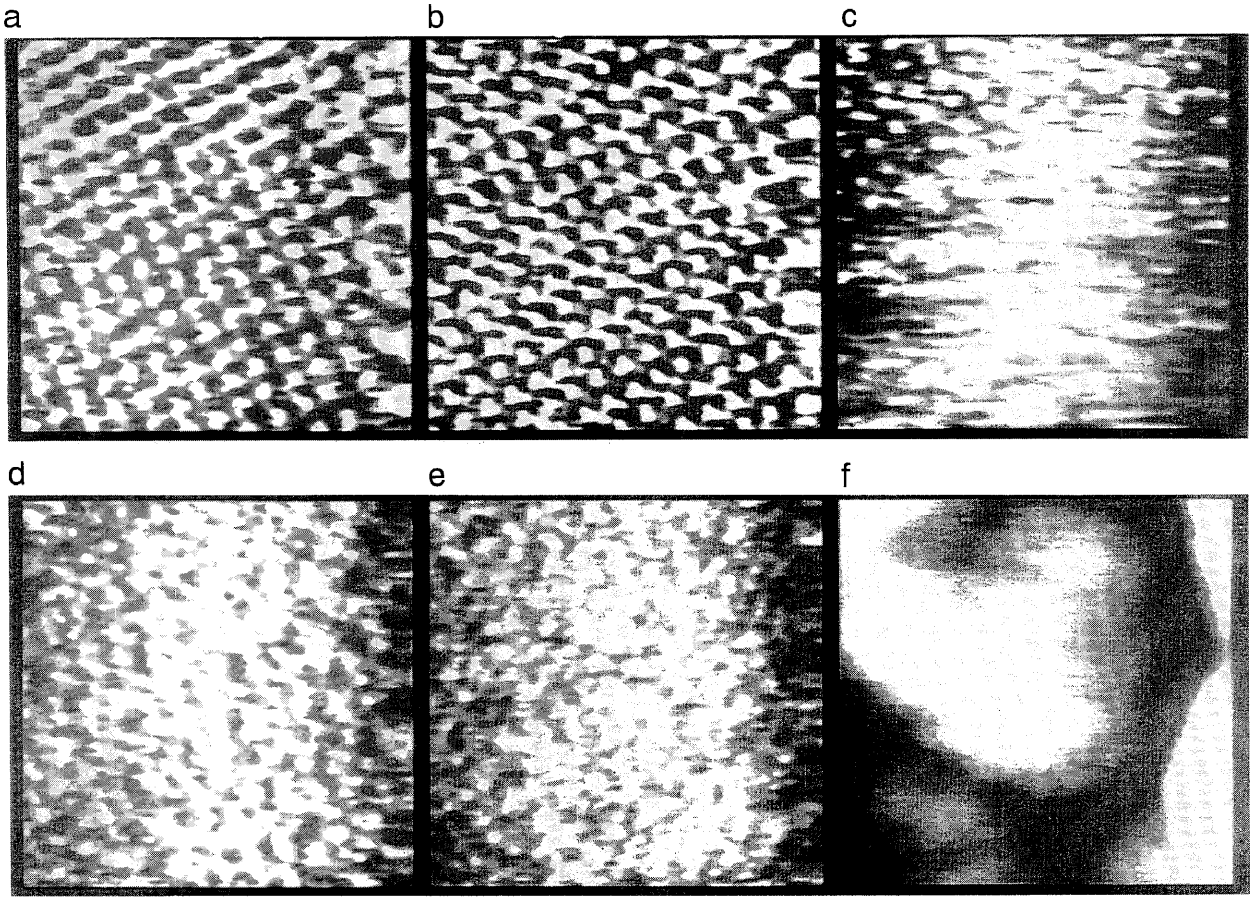

pounds (GIC). However in those cases, the measured heights (0.15nm and 0.05nm) were lower. Also the possibility of manipulation of individual adsorbate was not reported.

Figures 4a-4f show the STM images of $10\times10nm^2$ area for the bias voltages from +0.7V to -0.7V. Different types of modifications of the molecular arrangements were observed. Approaching first from positive bias towards -0.065V, process of transition from "ordered" state to "disordered" state in the ring arrangement took place. Finally, at -0.7V (minus on the sample relative to the probe), we could observe a quite different feature in the surface morphology. The oval and round shaped islands with the diameters going down to 5nm and 2nm in heights are shown to be the dominant features in Fig.5.

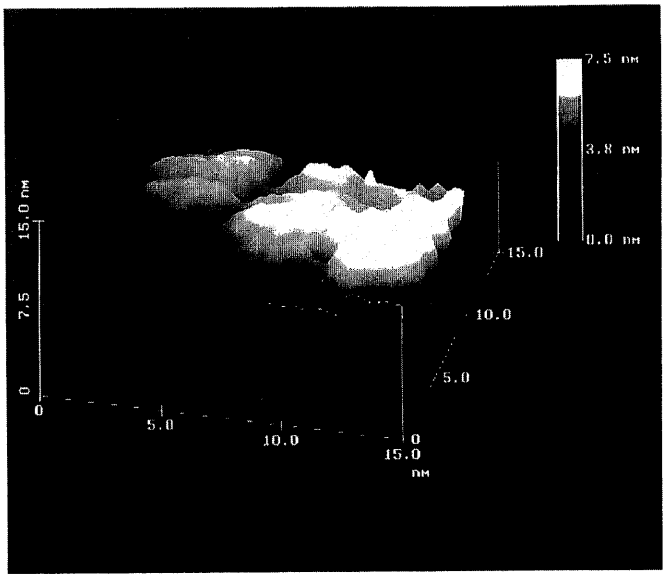

Figure 5. STM image of $15\times15nm^2$ area after applying -0.7V bias polarization.

It was not possible to obtain atomic resolution on the surface of the islands, but it seems that they are composed of smaller 0.5nm up to 1nm in diameter clusters. These islands are most probably identified as aggregates of selenium molecules or selenium atom chains after break down of the ring structure. The process of the phase change in the lattice system is not reversible with respect to the bias voltage.

In order to understand the structure and transformation observed by the STM, the first-principles calculations of the structure and electronic properties of Se_6 cluster have been carried out using DV-SCM method. The calculations are based on the density-functional theory(DFT) within the local density approximation(LDA) and linear combination of atomic orbitals. This method, discussed in detail elsewhere,[13),14)] has successfully been used in physics and chemistry of microclusters. The basis set is chosen to be the numerical form of the orbital solutions of self-consistent-field Kohn-Sham equation for the Se atom. Von Barth and Hedin's form of exchange-correlation potential is used.[15)]

The geometrical structure of Se_6 is optimized within the D_{3d} symmetry. We have obtained the optimized structure by surveying absolute minimum. Results are given in Table 1. From these coordinations of atoms, we know the 6 atoms form a six-membered ring hexametric molecules of 0.533nm in diameter and 0.21nm in height. It should be noted that in the calculation above we have taken the radius of Se-ion as 0.5Å.[16)] Although the calculated diameter is in good agreement with the result observed by STM, the calculated height is about 30% shorter than the one observed by STM.

Table 1. Coordinations of Atoms(Å)

No.	X	Y	Z	R
1	2.09854	0.00000	0.53482	2.16562
2	-1.04927	1.81739	0.53482	2.16562
3	-1.04927	-1.81739	0.53482	2.16562
4	1.04927	1.81739	-0.53482	2.16562
5	-2.09854	0.00000	-0.53482	2.16562
6	1.04927	-1.81739	-0.53482	2.16562

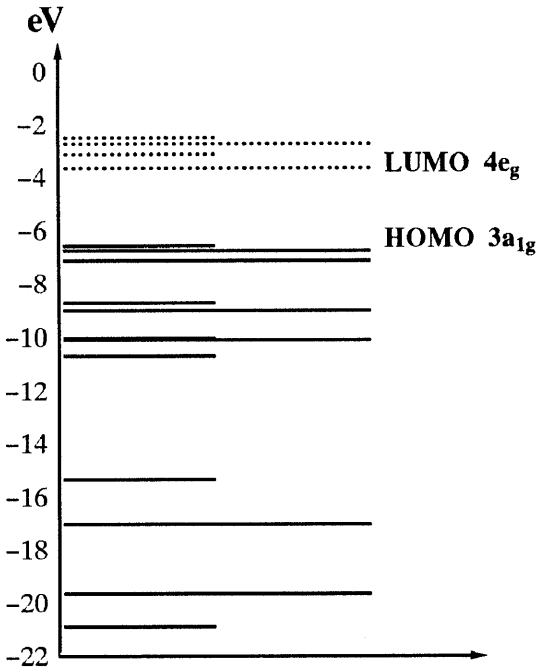

Figure 6. Electronic energy levels of the Se_6 ring cluster. Solid lines indicate the occupied states; dashed lines indicate unoccupied states.

In Fig.6, the calculated energy levels of the Se_6 cluster are given. The highest-occupied state of the Se_6 cluster is the $3a_{1g}$ state and is completely occupied by 2 electrons. The energy gap between the $3a_{1g}$ and the lowest unoccupied state, $4e_g$, is about 2.93eV. It is even larger than the energy gap of C_{60}. The analysis of the orbital overlap shows that the HOMO consists of strongly bonding orbitals and the LUMO antibonding, as is required for maximum stability of cluster. To get insight into the chemical bonding of Se_6, the density of states(DOS) of Se_6 cluster is shown in Fig.7. It is noticed that the p

electron states are around the Fermi level while the s electron states far below the Fermi level. The Mulliken population of Se_6 molecule is $4S_{1.93}4P_{4.07}$, close to that of free selenium atom. There are no much charge transfers between $s-$ and p-states. The present calculation shows Se_6 cluster is stable, because it has a very large HOMO-LUMO gap and a compact geometrical structure. The interaction among Se_6 molecules should be similar to that of C_{60} crystal, i.e. the van der Waals interaction.

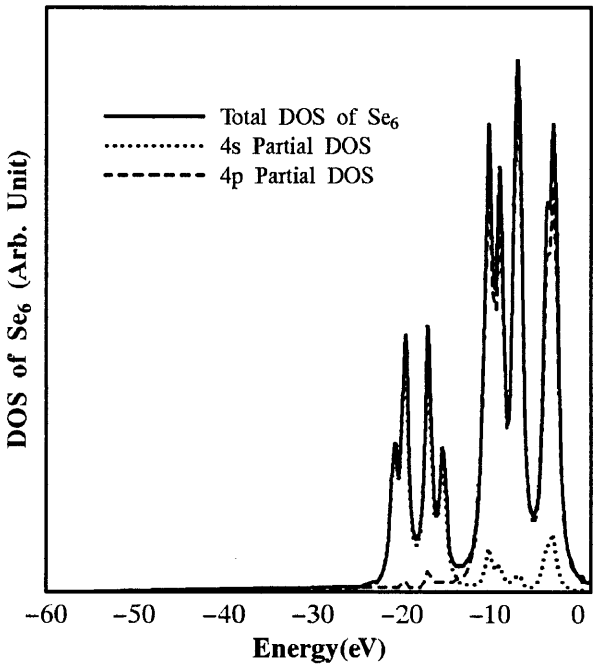

Figure 7. Density of states of Se_6 ring cluster. Solid line indicates the total density of states; dashed line indicates the $4s$ partial density of states and longer dashed line indicates the $4p$ partial density of states.

Table 2. Band Calculation Results

Binding energy of molecule Se_6	18.83(eV)
Binding energy per atom	3.12(eV)
Energy gap	2.93(eV)
Ionization potential(IP)	9.27(eV)
Symmetry	D_{3d} group

Table 2 gives a summary of the present band calculation. Binding energy of a Se_6 molecule is 18.83eV, i.e. 3.12eV per atom. The ionization potential is 9.27eV. As we know, when the bias voltage V_T=0.7V, the regular arrangement of two-dimensional Se_6 molecule crystal suddenly collapses to a random distribution of large clusters. From the present band structure calculation results, we can understand better the reason of the structural transformation. There are 6 valence electrons per atom, and these electrons are highly localized. The amount of energy increase ΔE in the electric field of V_T=0.7V is 4.2eV, it is larger than the binding energy of 3.12eV. Therefore, Se_6 molecules are broken and the two dimensional molecular crystal disappears. In fact, if a molecule gets 3.12eV energy, it should be broken, instead of 0.7V, the critical voltage for the transformation might be $\frac{3.12}{6} = 0.502$V. However, since there exists the tunnel current and the nonlocalized electrons in two dimensional lattice, the number of localized electrons per atom should be less than 6. From this point of view, the number of localized electrons per atom should be $\frac{3.12}{0.7} = 4.5$. The process of breaking molecule is not reversible because the charge voltage only can not repeat the process of reproducing Se_6 ring-type cluster.

From the point of view of industrial interest, the above mentioned phenomenon suggests the possibility of realizing the read-only memory with the two-dimensional densities of 10^3 to 10^5 times higher than conventional integrated circuits, since STM can manipulate individual clusters.

4. Conclusion

A rectangular monomolecular lattice arrangement of Se ring clusters has been obtained. These structures are stable in air conditions. By increasing the resolution, we hoped to determine whether such a ring arrangement can be an intercalant layer in GIC. Both cluster-cluster and cluster-substrate weak van der Waals interactions are important for forming monomolecular nanocluster lattice system. The nanometer-scale modification on these structures may be realized by changing both internal structure of clusters and their arrangement on the substrate by applying appropriate voltages and polarity of STM probe. The transformation at V_T=0.7V is due to the break of the ring-type molecule. The process of the phase change is not reversible.

A first-principles band calculation based on the DV-SCM method has been applied to these new experimental findings. The most stable structure obtained by the present calculation agrees well with the STM images. The stability of Se_6 ring-cluster is proved by the large value of HOMO-LUMO gap and the measured irreversible order-disorder transition caused by the STM needle is explained quantitatively using the estimated binding energies.

Acknowledgements

Authors would like to thank Prof. K. Suzuki (IMR, Tohoku University) and Prof. F. Hensel (Philipps-Universit Marburg) for valuable discussions. They would also like to thank Dr. A. Wawro for his assistance and discussion and the menbers of the Computer Science Group at the Institute for Materials Research for their assistance.

This work was support in part by New Program from the Ministry of Education Science and Culture in Japan and the Partnership Program with IBM Japan.

1) New Horizons in Low-Dimensional Electron Systems, ed. by H. Aoki, M. Tsukada, M. Schlutter and F. Levy, Kluwer Academic Publishers, Dordrecht Boston London, 1992.
2) N. Aoto, K. Sonouchi and A. Koma, Extended Abstracts of the 15th Conference of Solid State Devices and Materials, Tokyo, 1983, p.309
3) W. C. Cooper ed. Crystal growth and characterization in the physics of selenium and tellurium, Pergamon Press Oxford London, 1969, pp.87-223.
4) J. Becker, K. Rademann and F. Hensel, Z. Phys. D19(1991)229-231; (1991)233-235; Naturforsch., 46a(1991)453-461.
5) G. Binnig, H. Rohrer, Ch. Gerber and E. Whibel, Appl. Phys. Lett. 40(1982)178.
6) J. A. Stroscio and D. M. Eigler, Science 254(1991)1319.
7) Ph. Avouris and I.-W. Lyo, Appl. Surf. Sci. 60/61(1992)426.
8) U. Staufer, Surface Modification with a Scanning Proximity Probe Microscope (Scanning Tunneling Microscopy II, R. Wiesendanger and H.-J. Guntherodt (Eds.) Springer Series in Surface Sciences 28, Springer-Verlag Berlin Heildelberg New York 1992), pp. 273-302.
9) W. C. Cooper and R. A. Westury, The structure of Selenium, eds. R. A. Zingaro and W. C. Cooper, Van Nostrand Reinhold Co. New York, 1974, pp.86-147.
10) K. Nagata and Y. Miyamoto, J. J. Appl. Phys. 23(1984)704.
11) J. Mhlbach, P. Pfeu, E. Recknagel and K. Sattler, Surf. Sci. 106(1981)18.
12) D. Anselmetti, V. Geiser, G. Overney, R. Wiesendanger, H.-J. Guntherodt, Phys. Rev. B42(1990)1848; D. Anselmetti, V. Geiser, G. Overney, D. Brodbeck, R. Wiesendanger and H.-J. Guntherodt, Synth. Met. 38(1990)157.
13) B.-L. Gu and Z.-Q. Li, J. Phys. Condens. Matter 5(1993).
14) Z.-Q. Li and B.-L. Gu, Phys. Rev. B47, 13611(1993).
15) U. von Barth and L. Hedin, J. Phys. C5, 1629(1972).
16) Periodic Table of the Elements, ed. P. Lof, Elsevier Science Publishers B.V., 1987; A. F. Wells, Structural inorganic chemistry, Oxford University Press, Oxford, 1984, p.1382.